Simultaneous Heat and Mass Transfer with and without Reactant Exhaustion in Catalyst Particles for Reaction with Volume Change

Asymptotic analytic expressions for the concentration and temperature profiles as well as effectiveness factor inside porous, thin-disk shaped catalyst particles have been developed for zeroth-order exothermic reaction with reactant-to-product volume change. The individual and combinative effects of volume-change, Thiele and thermal Thiele moduli, and of the dimensionless activation energy are discussed. As expected, the expressions revert to those for the corresponding isothermal and constant-volume cases. Errors arising from the approximation were calculated and found to be quite acceptable.

MARSHALL M. LIH
and
KAN LIN

Department of Chemical Engineering
The Catholic University of America
Washington, D.C. 20017

SCOPE

The general objective of the authors' recent works has been to study the influence of volume or mole change on the mass transfer efficiency inside catalyst particles. In this paper, the heat transfer effect is included and the system studied is a zeroth-order exothermic reaction which frequently occurs in industrial practice such as the hydrogenation and dehydrogenation of cyclic hydrocarbons.

This reaction was chosen also because of the unique characteristic of zeroth-order reactions in exhibiting the reactant-exhaustion phenomenon which makes the interaction of heat and mass transfer highly interesting. However, because of mathematical complications, the simplifying approximation of moderate temperature rise has been made. However, analysis shows that the general applicability of the result is not seriously affected. The present study is also confined to thin-disk geometry.

The external heat and mass transfer across the film surrounding the catalyst particle is treated as a separate problem and thus not included here.

CONCLUSIONS AND SIGNIFICANCE

We have developed analytic solutions for the concentration and temperature profiles as well as for the effectiveness factor for zeroth-order reaction occurring in porous, thin-disk type catalyst particles with reactant-to-product volume change. Although an approximation was made, the error introduced is small enough to render the results useful in a large number of reaction systems, including such catalytic reactions as hydrogenation and dehydrogenation of cyclic hydrocarbons wherein the strong hydrocarbon adsorption allows the rate to be approximated by zeroth-order behavior.

The results show that the effectiveness factor decreases with increasing volume-change modulus (expansion) while it increases with increasing combination of the thermal Thiele modulus and dimensionless activation energy. However, the temperature profile inside the pellet does depend on the latter two factors separately. The study also confirms that when a reactant is exhausted before reaching the center of the pellet a flat temperature profile is maintained in this no-reaction central layer and the level of this temperature is a function of the thermal Thiele modulus (dimensionless heat generation-to-mass diffusion ratio) but not of the dimensionless activation energy. These dependencies and behaviors can be qualitatively applied to cylindrical and spherical particles as well.

In a recent series of papers (Lih and Lin, 1971; Lin and Lih, 1971, 1973) we have pointed out the important effect of the reactant-to-product volume change on the effectiveness of the catalyst particle as a diffusing medium. We have also developed analytic solutions for several reaction systems and found them to be highly systematic and interesting. However, they deal only with isothermal systems in which the heat consumed or released by the reaction is negligible. Consequently, there was no need to consider the heat transfer problem.

However, since a catalytic reaction is usually accompanied by heat generation or consumption and there is usually finite resistance to energy flow within the catalyst particle, a temperature gradient exists. This means that we should actually deal with heat and mass transfer simultaneously. This is the subject of the present paper. Since mass transfer determines concentration and heat

* K. Lin is with Gilbert Associates, Reading, Pa.

transfer determines temperature, and, consequently, the reaction rate constant, the combined action makes this study a fascinating one as many parameters interact.

Many investigators have studied the simultaneous heat and mass transfer problem. In most cases, except those considered by Weekman (1966) and Hlavacek and Kubicek (1971), however, the important effect of volume or mole change has been left out, probably because of the nonlinearity of the differential equation which would have resulted. But from our previous experience (Lih and Lin, 1971; Lin and Lih, 1971, 1973), we have developed sufficient confidence to deal with these nonlinear equations by transformation of variables.

To limit the scope of our study, we shall confine ourselves to exothermic reactions. As has been pointed out in classical works (Aris, 1965; Peterson, 1965) because of the heat released by such reactions, the reduction in reaction rate due to decreased concentration as the reactant attempts to diffuse toward the center could in some cases be more than offset by its increase due to increased temperature. The net effect is that the effectiveness factor could be higher than unity, as we shall see later in this paper. Also, since the effectiveness factor should approach unity as the Thiele modulus diminishes, the effectiveness factor exhibits a maximum while on both sides of it there could be two Thiele modulus values for each effectiveness factor. This interesting behavior is why exothermic reactions have occupied the attention of most workers in this field. Similar expressions can be developed for endothermic reactions but their effectiveness factor curves would simply parallel corresponding ones for isothermal cases, except at a lower level, that is, monotonically decreasing with increasing Thiele modulus.

BASIC ASSUMPTIONS

Before formulating the problem mathematically, let us set down the basic assumptions involved:

1. The catalyst particle has uniform catalytic activity and homogeneous pore structure and distribution throughout.
2. Mass transfer within the catalyst particle occurs by diffusion only and may be expressed by means of Fick's law of diffusion with a constant effective diffusivity.
3. Heat transfer within the catalyst particle occurs by conduction only and may be expressed by means of Fourier's law of heat conduction with a constant effective thermal conductivity.
4. The temperature dependence of reaction rate constant may be expressed by the Arrhenius law.
5. Values of heat of reaction and density of catalyst particle are constant when temperature change is relatively small.
6. The overall molal density (c) is position-independent, or constant.

ZEROTH-ORDER REACTIONS AND REACTANT EXHAUSTION

In this paper we shall confine ourselves to zeroth-order reactions because of the unique reactant-exhaustion phenomenon associated with this type of reaction. In nonzero, positive-order reactions the consumption of reactant(s) is accompanied by a corresponding decrease in the reaction rate so that the reactant will never be exhausted before the reaction ceases. The worst possibility is that both the reactant and the rate will vanish at the center of the catalyst particle.

However, a zeroth-order reaction proceeds at a constant rate regardless of concentration of reactant supply. Thus, it is possible that at some sufficiently high reaction rate the reactant (or one of the reactants) will run out before it has the chance to reach the center of the particle. We call the distance (from the center) at which this reactant is exhausted the exhaustion radius r_e or in dimensionless form $\xi_e = r_e/R$. Thus in conjunction with the equations of continuity and motion†

$$\left(\nabla^* \cdot \frac{1}{1+mC} \nabla^* C \right) = K_0^2 e^{\gamma\left(1-\frac{1}{y}\right)} \tag{13}$$

$$(\nabla^{*2} y) = -K_0^2 \beta e^{\gamma\left(1-\frac{1}{y}\right)} \tag{14}$$

we have the following sets of boundary conditions

[Case 1]
Reactant Exhausted at ξ_e

B. C. (1a) $\xi = 1 \quad C = 1$

(1b) $\xi = 1 \quad y = 1$

B. C. (2a) $\xi = \xi_e \quad C = 0$

(2b) $\xi = \xi_e \quad y = y_{max}, \quad \dfrac{dy}{d\xi} = 0$

[Case 2]
Reactant Not Exhausted

(1'a) $\xi = 1 \quad C = 1$

(1'b) $\xi = 1 \quad y = 1$

(2'a) $\xi = 0 \quad \dfrac{dC}{d\xi} = 0$

(2'b) $\xi = 0 \quad \dfrac{dy}{d\xi} = 0$

It should be noted that despite the zeroth-order limitation, the present analysis finds many applications because the condition is frequently encountered in the hydrogenation or dehydrogenation of cyclic hydrocarbons where strong adsorption of the hydrocarbon on the catalytic surface reduces the Hougen-Watson type rate equation to one of the zeroth order. Examples include benzene hydrogenation on supported metals and some hydroisomerization reactions.

RESULTS FOR THIN-DISK GEOMETRY

To further limit the scope of this work, let us consider only the thin-disk (or flat-plate) type of catalyst particles. This limitation, however, does not prohibit the application of the qualitative arguments of this work to other geometries such as cylinders and spheres, although the precise results are naturally different.

Using the variable transformation

$$\psi(C) = \frac{1}{m} \ln (1 + mC) \tag{15}$$

and the assumption that temperature rise in the particle

† For detailed mathematical derivation and equation numbering, a supplement has been deposited as Document No. 02161 with the National Auxiliary Publication Service (NAPS), c/o Microfiche Publications, 305 E. 46 St., N.Y., N.Y. 10017 and may be obtained for $1.50 for microfiche or $5.00 for photocopies.

TABLE 1. SUMMARY OF ASYMPTOTIC ANALYTIC SOLUTIONS FOR THIN-DISK GEOMETRY

	Reactant exhausted at $\xi = \xi_e$		Reactant not exhausted	
Concentration profile, $C^\Delta = \frac{c_A}{c_{AS}}$	$\frac{1}{m}\left\{\{\cosh[D(\xi-\xi_e)]\}^{2m/\beta\gamma}-1\right\}$	(34)	$\frac{1}{m}\left[(1+m)\left(\frac{\cosh D_0\xi}{\cosh D_0}\right)^{2m/\beta\gamma}-1\right]$	(42)
Temperature profile, $y^\Delta = \frac{T}{T_s}$	$1+\alpha\beta-\frac{2}{\gamma}\ln\cosh[D(\xi-\xi_e)]$	(35)	$1+\frac{2}{\gamma}\ln\frac{\cosh D_0}{\cosh D_0\xi}$	(43)
Effectiveness factor, η^Δ	$\frac{2D}{\delta}\tanh[D(1-\xi_e)]$	(36)	$\sqrt{\frac{2P}{\delta}}\tanh\sqrt{\frac{\delta P}{2}}$	(45)
Where	$D=\sqrt{\frac{\delta}{2}}(1+m)^{\beta\gamma/2m}$	(37)	$D_0=D(\xi_e=0)=\sqrt{\frac{\delta P}{2}}$	
	$\delta = K_0^2\beta\gamma$	(23)		
			$P=\cosh^2\sqrt{\frac{\delta P}{2}}$	(44)
	$\xi_e = 1-\frac{1}{D}\cosh^{-1}D\sqrt{\frac{2}{\delta}}$	(31)		
	$K_0=\sqrt{\frac{2}{\beta\gamma}}\frac{\cosh^{-1}(1+m)^{\frac{\gamma\beta}{2m}}}{(1+m)^{\frac{\gamma\beta}{2m}}(1-\xi_e)}$	(39)		

The reader will note that the formulas in the right-hand column can be obtained from corresponding ones in the left-hand column by setting $\xi_e = 0$. Interrelationships among D, P, δ, and ξ_e are graphically given in Figure 1. Sometimes it is more convenient to use Figure 2, a cross-plot of Figure 1, because in most applications D and δ are usually calculated before ξ_e is.

$\Theta/\gamma\left(=\frac{T-T_s}{T_s}\right)$ is small or moderate, the resulting formulas for concentration and temperature profiles and for the effectiveness factor for both the cases of reactant exhaustion and nonexhaustion can be summarized in Table 1.

GRAPHICAL REPRESENTATION

The asymptotic analytic solutions for concentration and temperature distributions and effectiveness factor are plotted in Figures 3 through 11 showing effects of m, ξ_e, K_0, β, and γ.

Note that in most of the equations derived [Equations (34), (36), (42), and (45)], β and γ appear together as a product. Accordingly, we can plot $\beta\gamma$ as a single combined parameter thus saving unnecessary charts (see Figures 3, 5, 7, 10 and 11). Indeed, the effects of β and γ are the same as far as mass transfer is concerned, as will be seen in the Discussions.

It should also be noted that the reactant-exhaustion and nonexhaustion cases can be plotted on the same graph because the latter is merely an extension of the former, that is, when $\xi_e = 0$.

From Equations (36) and (37) we can see that the effectiveness factor η^Δ can be expressed in terms of ξ_e via m at a certain value of $\beta\gamma$. This we have plotted in Figure 10 as the family of curves on the left. Conversely, if we regard ξ_e as a function of K_0, [Equations (23) and (31)], we can also plot η^Δ vs. K_0 for the various m values, as the family of curves on the right. Then we can also directly relate K_0 to ξ_e as indicated by the dotted path, which is what Equation (39) says analytically.

DISCUSSIONS

The above series of equations and charts offer many interesting features and principles which would otherwise be buried without the mathematical analysis. We shall enumerate them one by one.

1. The expressions developed for zeroth-order reactions occurring in thin-disk catalyst particles involve an approximation ($\Theta/\gamma \to 0$). They should be directly applicable to the situation prescribed, that is, small or moderate temperature rise. The error arising from using the approximation in obtaining Equation (36) or (37) increases with increasing β, m, and Θ/γ as expected. In the extreme case of $\beta = 0$, for example, no approximation is needed and we already have the exact analytic

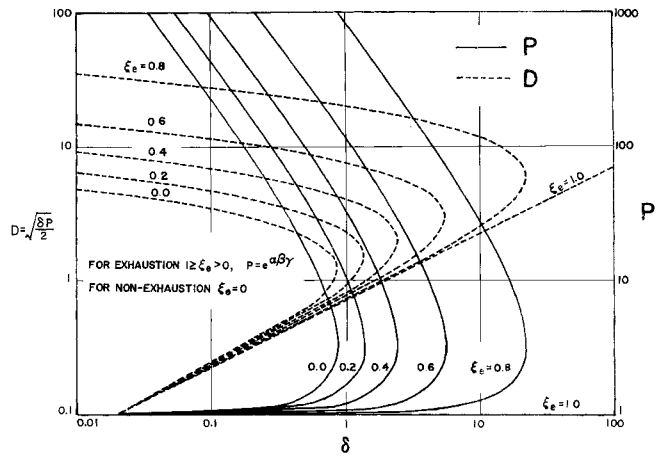

Fig. 1. Dependence of D and P on δ at various ξ_e. Note that D and P can be directly related as shown by the arrowed lines. It also applies to cases without reactant exhaustion ($\xi_e = 0$), see Case 2.

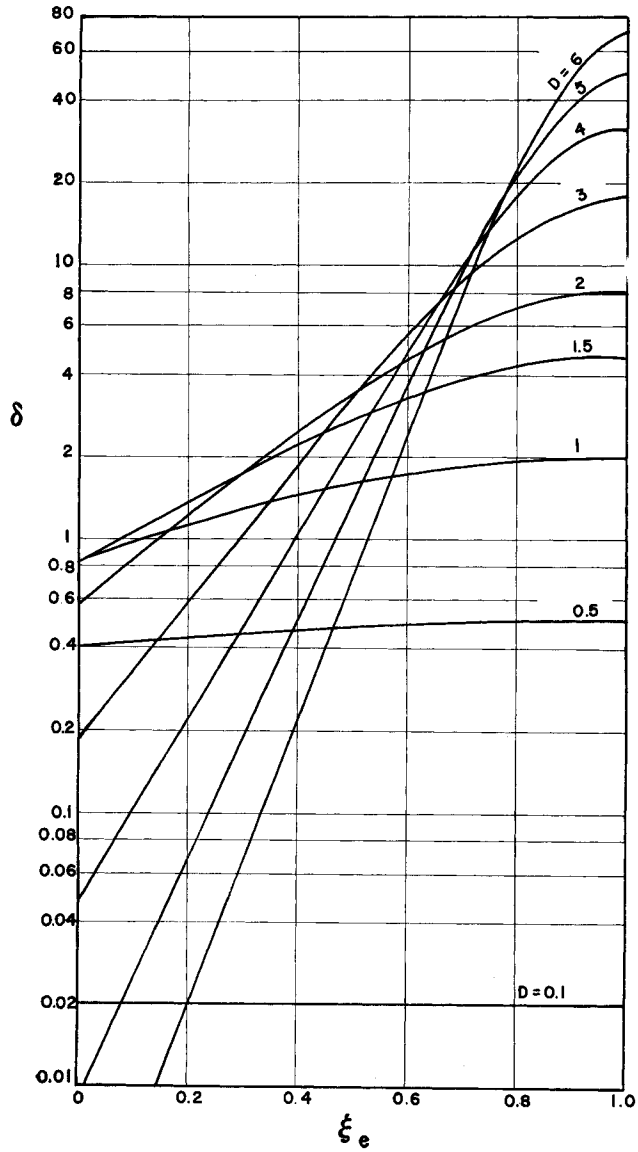

Fig. 2. Dependence of δ on ξ_e at various D values.

solution for that (Lin and Lih, 1971). For practical values of β, m, and γ, the error on the effectiveness factor is below 20% in the reactant exhaustion regime ($K_0 > K_{0e}$) and is essentially independent of the Thiele modulus, K_0; that is, asymptotic and exact effectiveness factors appear as parallel straight lines on the log-log η^{Δ} vs K_0 plot. In the nonexhaustion regime, especially for $K_0 < 0.5$, the error of the asymptotic solution compared with the exact one is always less than 4%. These errors are all positive; that is, the asymptotic value is always larger than the corresponding exact one. For $K_0 < 0.1$, the error practically vanishes.

2. The criterion for whether or not the reactant will

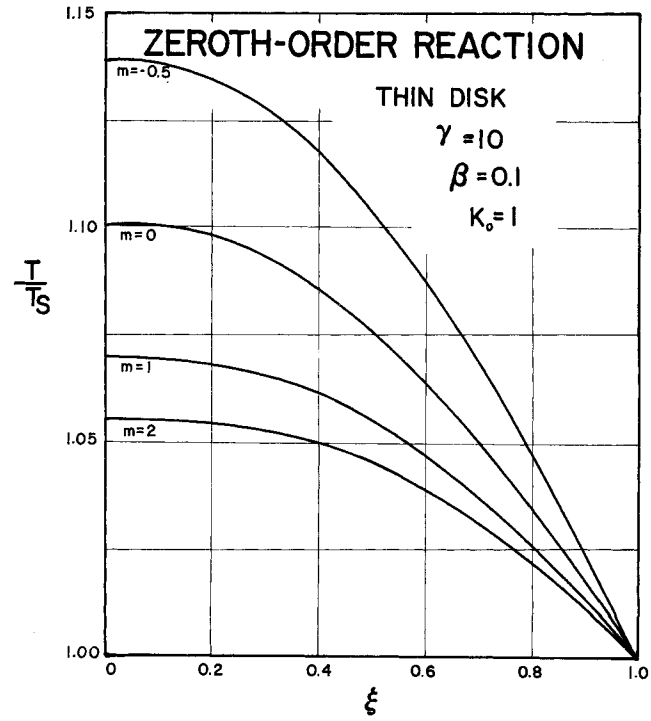

Fig. 4. Effect of volume-change modulus on temperature profiles; zeroth-order exothermic reaction, thin disk.

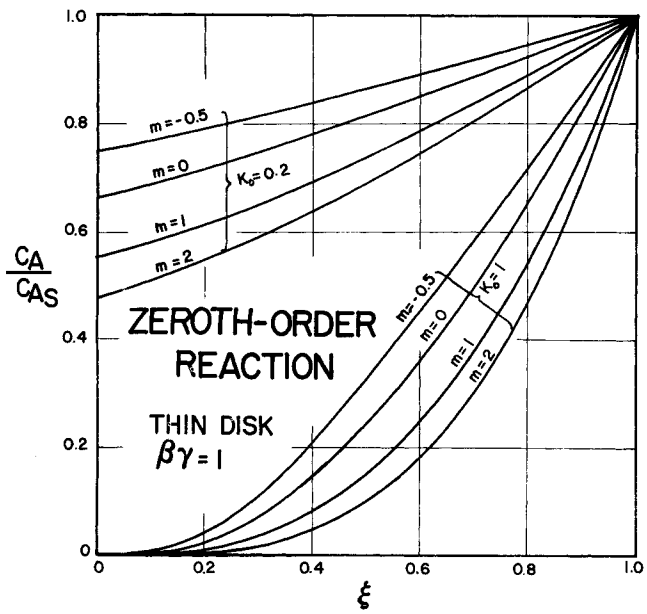

Fig. 3. Effect of volume-change modulus on concentration profiles; zeroth-order exothermic reaction, thin disk.

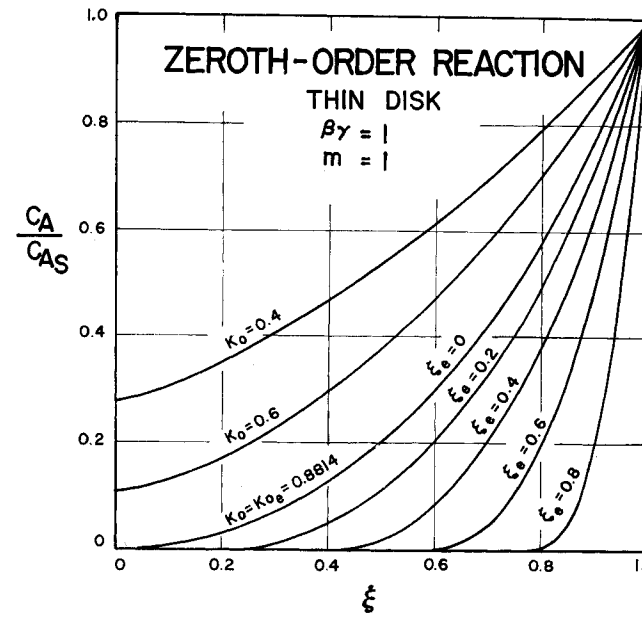

Fig. 5. Concentration profiles for zeroth-order exothermic reaction at various Thiele moduli and exhaustion depths, thin disk.

be exhausted before reaching the center of the catalyst particle can be established by requiring $\xi_e = 0$ in Equation (39)

$$K_{0e} = \sqrt{\frac{2}{\beta\gamma}} \cdot \frac{\cosh^{-1}(1+m)^{\frac{\beta\gamma}{2m}}}{(1+m)^{\frac{\beta\gamma}{2m}}} \qquad (46)$$

3. A closer examination of the equations and figures shows that while the concentration profile and effectiveness factor are dependent upon $\beta\gamma$ as a combination (product), as pointed out in the last section, the temperature profile does depend on β and γ separately (see Equations (35) and (43), Figures 8 and 9). This may seem strange at first, but careful consideration shows that this is reasonable because the temperature distribution should certainly depend on the heat released by the reaction ΔH_A. This is where β comes in. However, in order to affect the reaction rate and thus the effectiveness factor and concentration profile, it must go through γ, the dimensionless activation energy which is a measure of temperature sensitivity. Thus, if the large amount of heat released (β) by a certain reaction is offset by a low temperature sensitivity (γ), the net effect could remain to be quite moderate. In the extreme case when $\gamma = 0$, the reaction rate is not dependent upon temperature; hence the effectiveness factor and concentration profile remain constant regardless of the amount of heat released. For the effectiveness factor and concentration profile this case would be identical to that of no heat generation ($\beta = 0$) although the temperature profile is an entirely different story.

4. Accordingly we can verify, for example, Equation (46) by setting $\beta = 0$ or $\gamma = 0$, or both, to show that for the critical Thiele modulus it indeed reverts to the isothermal case (Lin and Lih, 1971) in which the critical Thiele modulus K_{0e} is equal to

$$\sqrt{2j\frac{\ln(1+m)}{m}}$$

Many other expressions can be reduced to the corresponding ones for isothermal cases in like manner.

5. The above point can be extended to graphical rep-

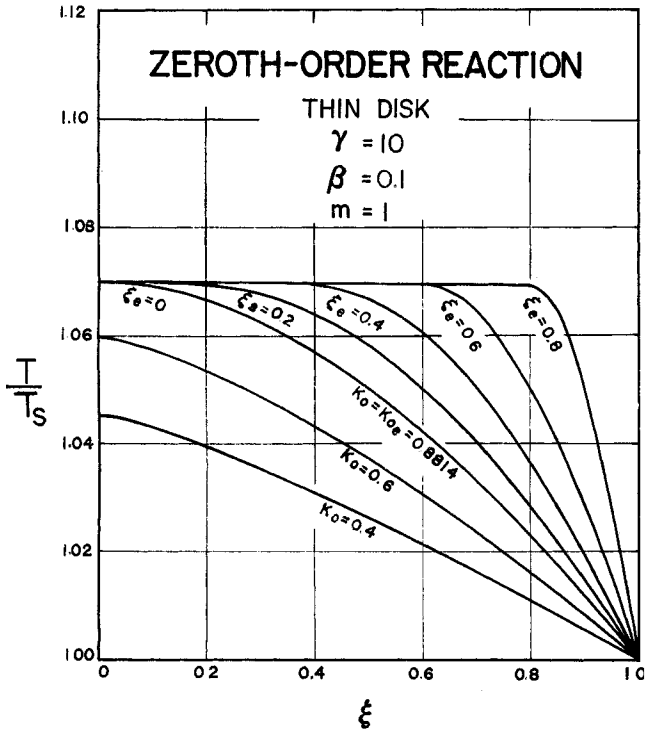

Fig. 6. Temperature profiles for zeroth-order exothermic reaction at various Thiele moduli and exhaustion depths, thin disk. Note that as long as there is reactant exhaustion the maximum center-layer temperature does not change with the thickness of this no-reaction zone.

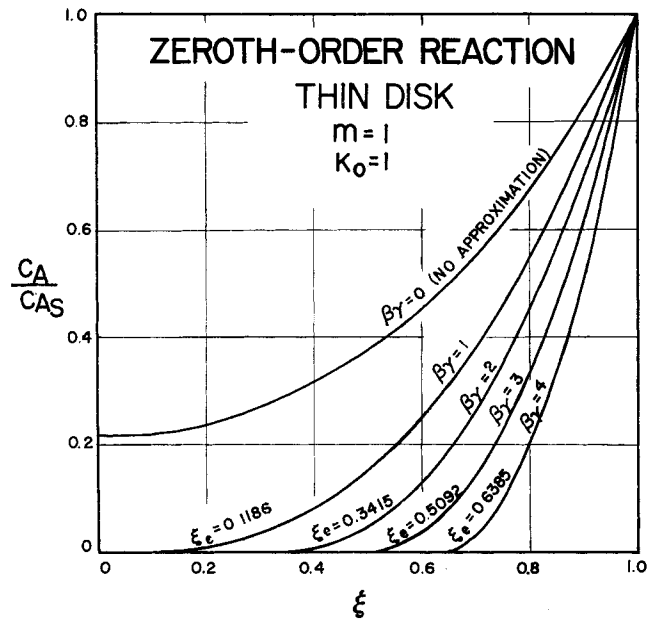

Fig. 7. Concentration profiles for zeroth-order exothermic reaction at various $\beta\gamma$ values, thin disk. Note that exhaustion depth changes with $\beta\gamma$ values.

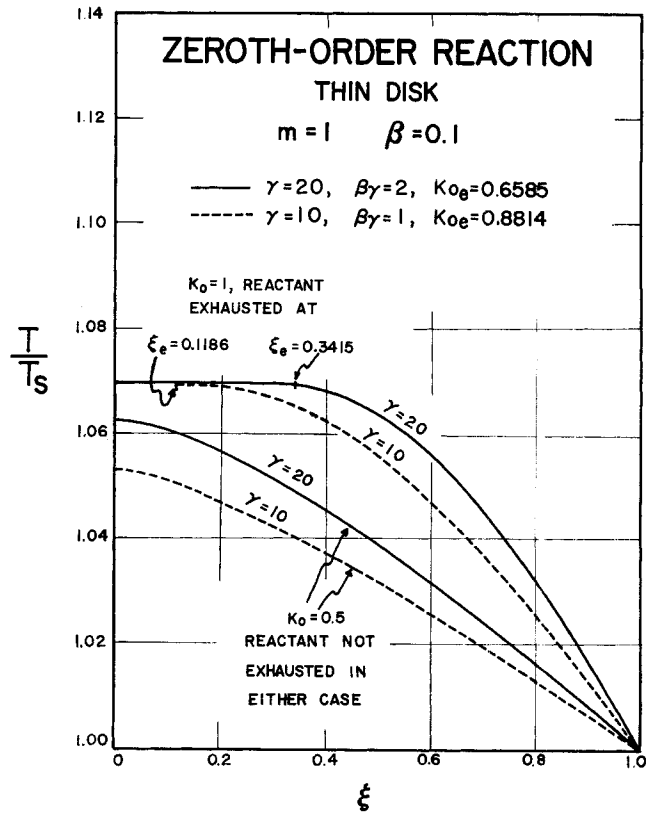

Fig. 8. Temperature profiles for zeroth-order exothermic reaction at various dimensionless activation energy, γ, values. Note that when there is exhaustion, the maximum temperature at the no-reaction zone is always the same regardless of γ.

resentation such as shown in Figures 5 and 6 which we can divide into two regions. For $K_0 < K_{0e}$, we have plotted the concentration and temperatures profiles at different K_0 values. Above K_{0e}, at which we note that the concentration goes to zero at $\xi_e = 0$, the more important factor is ξ_e. Thus we have plotted the profiles at various ξ_e values instead of K_0's.

6. To ponder the meaning of these graphs further, we note that above $K_0 = K_{0e}$ an interesting phenomenon occurs. That is, regardless how much we increase K_0 and thus ξ_e, the temperature at the center does not increase anymore. In fact, the isothermal layer* at the center expands with increasing K_0 and ξ_e. This has actually been predicted when we made the assumption of y_{max} (B. C. 2b Case 1, see Appendix.† The present result confirms it.

7. The same can be said of the effect of γ. Figure 8 shows that as long as there is reactant exhaustion at ξ_e, we always have the same uniform maximum (core or center-layer) temperature, regardless of how thick this no-reaction layer is. However, if either K_0 or γ drops to such an extent that reactant is no longer exhausted anywhere, γ will have a definite effect on the temperature at the center-plane.

8. However, the same cannot be said of the effect of β (Figure 9). Whether or not reactant is exhausted, the heat released by a reaction does have a definite effect on the temperature level inside the catalyst particle.

9. The value of $(1 + m)^{\beta\gamma/2m}$ has to be greater than or equal to unity, in order to fulfill the requirement of the argument of inverse hyperbolic cosine appearing in Equation (39). This is automatically satisfied because if

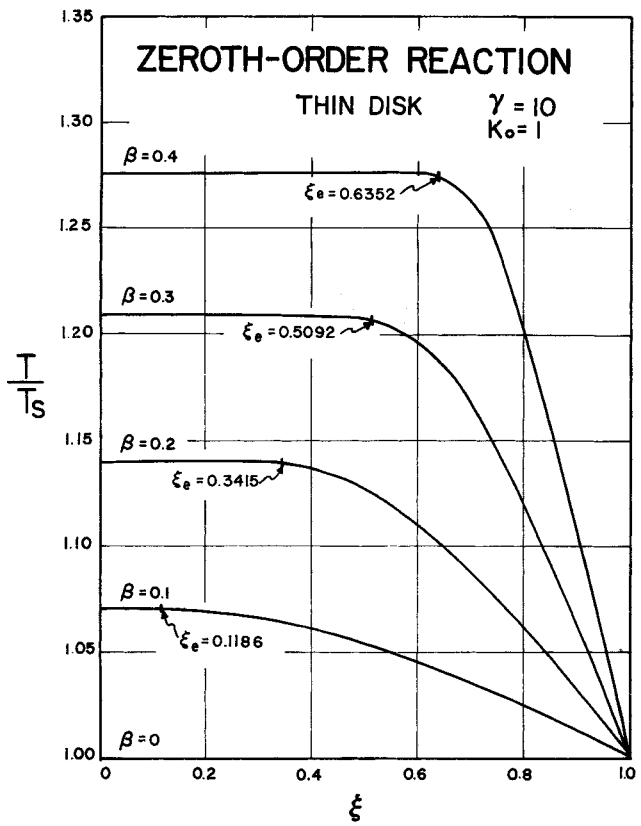

Fig. 9. Temperature profiles for zeroth-order exothermic reaction at various β values, thin disk. Note where reactant exhaustion occurs.

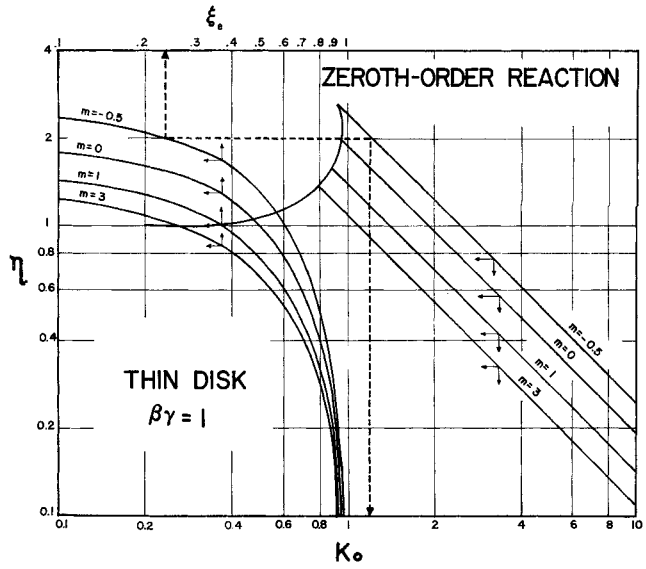

Fig. 10. Effectiveness factor vs. Thiele modulus and reactant-exhaustion depth at different volume-change moduli; zeroth-order exothermic reaction, thin disk. Note that ξ_e can be directly related to K_0 as indicated by the dotted lines.

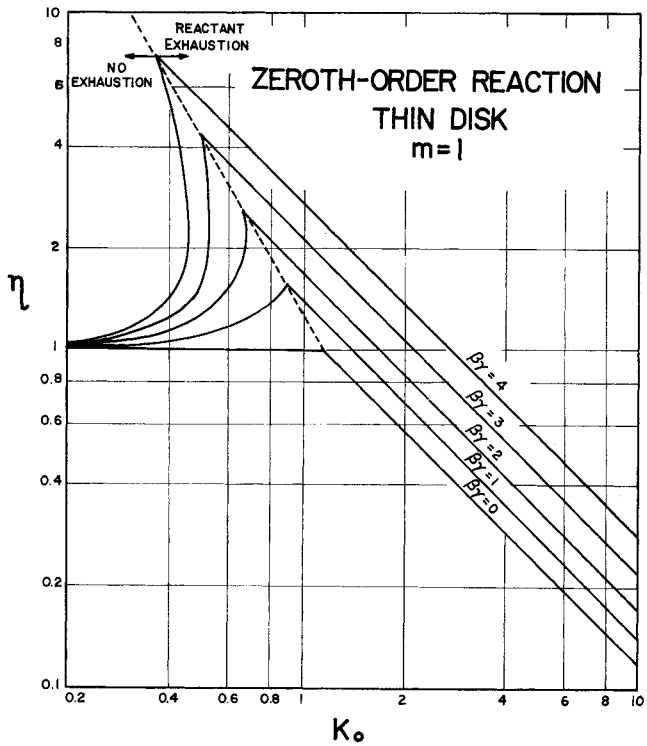

Fig. 11. Effectiveness factor vs. Thiele modulus for zeroth-order exothermic reaction at different $\beta\gamma$ values, thin disk. Note that the chart is divided into reactant-exhaustion and no-exhaustion regions by the locus of the maximum effectiveness factors.

m is positive, $(1 + m)^{\beta\gamma/2m}$ is greater than unity since $\gamma\beta/2m$ is also positive. On the other hand, if m is negative $(-1 < m < 0)$,* $\gamma\beta/2m$ is also negative, also making $(1 + m)^{\gamma\beta/2m}$ greater than unity. When $m = 0$, $(1 + m)^{\gamma\beta/2m} = 1$ again satisfying the same requirement.

10. It can also be shown that the equations derived herein can be reduced to the ones without volume change

* For cylindrical and spherical cases, this would be a center "rod" and "core", respectively.

† See footnote on page 833.

* m cannot be smaller than −1 since at m = −1 we would have infinite contraction, a physical impossibility.

(Hlavacek and Marek, 1968) by setting $m = 0$.

11. From the effectiveness factor charts, (Figure 10 and 11), we can see that the effectiveness factor increases with decreasing Thiele modulus by virtue of a larger reaction zone because of a smaller exhaustion radius when there is reactant exhaustion. [For thin-disk and on log-log plot, it does linearly. For cylindrical and spherical geometries, linearity is not expected to hold. See corresponding isothermal cases in Lin and Lih (1971)]. It even increases beyond $\eta^{\Delta} = 1$ to such a point that the reactant is no longer exhausted ($\xi_e = 0$). Further decreasing the Thiele modulus would only mean a decrease in reaction rate (rate constant times the area; note that the diffusion and concentration have no consequence as long as reactant fills up everywhere) and thus reduced effectiveness factor. This ultimately reaches $\eta = 1$ for extremely small K_0. Therefore, a very important conclusion here is that maximum effectiveness factor occurs right at the borderline between reactant exhaustion and nonexhaustion, unlike in isothermal cases where η reaches a plateau of $\eta = 1$ at $\xi_e = 0$ and stays at this maximum even when K_0 is further reduced.

12. This maximum appears to increase linearly with decreasing K_0 on this log-log plot. However, this cannot be verified from Equations (36) and (37).

13. The locus of these maxima divides the chart into two regimes. To the right is where reactant will be exhausted at ξ_e while on the left it will never be exhausted, as shown in Figure 11.

14. Equations (36) and (37) shows that for reactant-exhaustion cases, the effectiveness factor is a function of m; this is borne out by the graph (Figure 10). For no-exhaustion cases, on the other hand, Equation (45) dictates that there be only one curve, regardless of the m value. This is again verified in Figure 10. In fact, since the no-exhaustion case starts where the exhaustion case ends, the single no-exhaustion curve can be obtained by joining the ends of the exhaustion lines for the various m values.

15. It should be mentioned that external heat and mass transfer effects are also important and they interact with the internal transport processes. However, in the present paper we follow the classical approach and consider them a separate step (see, for example, Peterson, 1965; Chapts. 4 and 6). Their effects can be linked to those of the internal heat and mass transfer through the surface concentration c_{AS} and temperature T_s and thus are not discussed in details here. In the work of Hlavacek and Kubicek (1971), the internal and external transport processes are connected via the interphase transport coefficients in the form of Nusselt and Sherwood numbers.

ACKNOWLEDGMENTS

This study was supported by the Petroleum Research Fund (GF-895) administered by the American Chemical Society and Grant No. GU-3285 of the National Science Foundation. Computer time and facilities were provided by the Computer Center of the Catholic University of America.

NOTATION

A' = frequency factor
a = catalytic surface area per unit volume of catalyst
b = stoichiometric coefficient in reaction $A \rightarrow bB$
c = total molal concentration of mixture
$C = \dfrac{c_A}{c_{AS}}$, dimensionless concentration
c_A = local molal concentration of species A
$D = \sqrt{\dfrac{\delta}{2}}\,(1+m)^{\frac{\gamma\beta}{2m}} = \sqrt{\dfrac{\delta}{2}}\,e^{\alpha\beta\gamma/2}$
$D_0 = \sqrt{\dfrac{\delta P}{2}}$
D_{eff} = effective diffusivity of A in porous catalyst particle
E = molal activation energy of reaction
$-\Delta H_A$ = heat of reaction (produced per mole of A reacted)
j = geometric index (= 1, 2, 3, for thin-disk, infinite cylinder and sphere, respectively)
$K_n = \dfrac{D}{2}\sqrt{\dfrac{k_{ns}\,a\,c_{AS}{}^{n-1}}{D_{\text{eff}}}}$, Thiele modulus for nth-order reaction
k_n = rate constant for nth-order reaction of type $A \rightarrow bB$
k_{ns} = rate constant evaluated at temperature T_s
m = $(b-1)x_{AS}$, volume-change modulus
N_i = total molal flux of species i, moles/(time)(area)
n = order of reaction, positive integer
P = integration constant
q = energy flux
Q = integration constant
R = gas constant
R_i = molal production rate of species i
r = radial coordinate
S = external surface area
T = absolute temperature
T_s = temperature at geometric surface of particle
V = total volume of catalyst particle
x_i = molar fraction of species i in mixture
$y = \dfrac{T}{T_s}$, dimensionless temperature

Greek Letters

$\alpha = \dfrac{1}{m}\ln(1+m)$
$\beta = \left(\dfrac{\theta_n}{K_n}\right)^2$
$\gamma = \dfrac{E}{RT_s}$, dimensionless activation energy
$\delta = K_0{}^2\,\beta\gamma$
λ_{eff} = effective thermal conductivity
η = effectiveness factor
$\theta_n = \dfrac{D}{2}\sqrt{\dfrac{k_{ns}\,a\,c^n{}_{AS}(-\Delta H_A)}{\lambda_{\text{eff}}\,T_s}}$
$\theta = \gamma\beta\,(\alpha - \psi)$
ξ = dimensionless radial coordinate, or, in case of thin disk, coordinate from centerplane
ξ_e = dimensionless radial distance at which the reactant disappears
$\psi = \dfrac{1}{m}\ln(1+mC)$
∇ = vector differential operator
$\nabla^* = \dfrac{D}{2}\nabla$, the dimensionless differential operator

Superscripts

Δ = with volume change
* = dimensionless

Subscripts

A = reactant A
B = product B
e = reactant exhausted
n = nth-order reaction

r = radial
s = surface

LITERATURE CITED

Aris, R., "Introduction to the Analysis of Chemical Reactors," p. 140, Prentice-Hall, Englewood Cliffs, N. J. (1965).

Bird, R. B., W. E. Stewart, and E. N. Lightfoot, *Transport Phenomena*, pp. 245 & 502, Wiley, New York (1960).

Frank-Kamenetzky, D. A., "Diffusion and Kinetics of Heterogeneous Reactions," *Acta Physicochim. U.R.S.S.*, **16**, 357 (1942).

Hlavacek, V., and M. Kubicek, "Modelling of Chemical Reactors. XXIII. Transient Heat and Mass Transfer in a Porous Catalyst. III. Reaction with Finite Values of Sherwood and Nusselt Numbers. Effect of Volume Contraction," *J. Catal.*, **22**, 364 (1971).

Hlavacek, V., M. Marek, and M. Kubicek, "Modelling of Chemical Reactors: VII. Heat and Mass Transfer in a Particle of Porous Catalyst. Zero-Order Reactions-Numerical Results," *Collect. Czech. Chem. Commun.*, 33 (3), 718 (1968).

Lih, M. M., and Lin, K., "Concentration Profiles and Effectiveness Factor in Catalyst Particles with Reactant-to-Product Volume Change: First-Order Kinetics," *J. Chinese Inst. Chem. Engrs.*, 2(1), (1971).

Lin, K., "Effectiveness Factor in Catalytic Reactions with Volume Change," Ph.D. dissertation, Catholic U. of America, Washington, D. C. (1970).

———., and Lih, M. M., "Concentration Distribution, Effectiveness Factor, and Reactant Exhaustion for Catalytic Reaction with Volume Change," *AIChE J.*, **17**, 1234 (1971).

———., "Effectiveness Factor for Catalytic Reactions of Arbitrary Order and with Volume Change," to be published.

Parks, J. R., "Criticality Criteria for Various Configurations of a Self-Heating Chemical as Functions of Activation Energy and Temperature of Assembly," *J. Chem. Phys.*, **34**, 46 (1961).

Peterson, E. E., *Chemical Reaction Analysis*, § 4.4 Prentice-Hall, Englewood Cliffs, N. J. (1965).

Weekman, V. W., Jr., "Combined Effect of Volume Change and Internal Heat and Mass Transfer on Gas-Phase Reactions in Porous Catalysts," *J. Catal.*, **5**, 44 (1966).

Manuscript received June 13, 1972; revision received February 16 and accepted February 17, 1973.

Dropwise Condensation Phenomena

Dropwise condensation of water vapor on long vertical tubes was investigated as to in situ cleaning and promoting techniques for a variety of tube materials.

Excess promoter on the tube surface significantly reduces heat transfer but appears to be slowly removed by draining.

Measured steamside heat transfer coefficients for copper, gold, Admiralty, Cu-Ni 90-10, and Monel tubes are adequately correlated by the theory of Mikic (1969) modified to include the effect of wall thickness.

A photographic study revealed that falling drops are elongated into rivulets on long vertical surfaces. Short (<65 mm) rivulets and small, barely visible drops over most of the area are evidence of excellent dropwise condensation.

DAVID G. WILKINS
and
LEROY A. BROMLEY

Department of Chemical Engineering
University of California
Berkeley, California 94720
and
The Bodega Marine Laboratory
University of California
Bodega Bay, California 94923

SCOPE

Heat transfer can be greatly improved by condensing vapor as discrete drops rather than as a continuous film. Dropwise condensation of water vapor is achieved by applying an organic compound to render the surface nonwetting. Promoter life is short under industrial conditions mainly due to fouling. One of the objectives of this study was to find more effective cleaning and promoting techniques for a variety of tube materials, especially the more corrosion-resistant alloys. Testing was done in a single tube apparatus and a five-effect Multiple Effect Flash Evaporator (Bromley and Read 1970).

Steamside heat transfer coefficients with dropwise condensation have been reported by others for copper, zinc, and stainless steel and were found to be dependent upon the thermal conductivity of the tube material. Two disparate theories have been advanced to explain this phenomenon. The validity of these theories was tested by measuring dropwise heat transfer coefficients for a variety of tube materials.

Correspondence concerning this paper should be addressed to L. A. Bromley. D. G. Wilkins is with U. S. Borax Research, Boron, California 93516.